



# OPEN Relative importance of soil fertility and microtopography as CO<sub>2</sub> and CH<sub>4</sub> exchange drivers in a northern boreal fen ecosystem

Juha Mikola<sup>1,2,✉</sup>, Sari Juutinen<sup>3</sup>, Aleksi Räsänen<sup>4,5</sup>, Tarmo Virtanen<sup>6</sup>, Timo Penttilä<sup>1</sup>, Hanna Hyvönen<sup>6</sup>, Lauri Heiskanen<sup>1,3</sup> & Mika Aurela<sup>3</sup>

While peatland C cycling is generally well covered, understanding of the role of soil fertility in driving the spatial variation of C fluxes within peatlands remains scattered. Our aim was to examine the relative effects of fertility and microtopography on CO<sub>2</sub> and CH<sub>4</sub> exchange within a boreal fen and to link these effects to the spatial variation in plant and soil attributes. Fertility zones (eutrophic, mesotrophic, oligotrophic) were judged by moss species appearances, and the growing season CO<sub>2</sub> and CH<sub>4</sub> exchange was measured by static chambers for microforms (string, *Sphagnum* lawn, flark) and fertility zones and by eddy covariance technique for the entire ecosystem in three years. Plant leaf area index, plant functional type biomasses, soil C and N concentrations and litter decomposition were measured at study plots placed on the microforms and fertility zones. We found that higher fertility led to greater fluxes in both gases: the eutrophic zone had 111% higher net ecosystem CO<sub>2</sub> exchange, 102% higher gross primary production, 83% higher ecosystem respiration and 93% higher CH<sub>4</sub> emissions than the oligotrophic zone. Peat N concentration was lowest in the eutrophic zone, indicating fast N cycling. The relative importance of microtopography and fertility differed between the two gases: while microform explained 31–39% and fertility 10–15% of total variation in CO<sub>2</sub> exchange, microform explained 14% and fertility 36% of variation in CH<sub>4</sub> exchange. These results show that growing season CO<sub>2</sub> and CH<sub>4</sub> fluxes can be significantly affected by within-fen variation of fertility and that CH<sub>4</sub> emissions can be more closely associated with fertility than microtopography. It seems that understanding of within-site variation in soil nutrient availability is highly relevant for predicting current and future C exchange in peatlands.

**Keywords** Aapa mire, Litter decomposition, N cycling, Microform, Spatial variation

In terms of global carbon (C) cycling, the significance of peatlands lies in their ability to accumulate extensive amounts of C in their soil. Northern latitudes above 30° N contain 91% of the global peatland area, and this is where 89% of peatland C is stored<sup>1</sup>. In the global north, peatlands have acted as a continuous C sink since the last deglaciation<sup>1,2</sup>, and even at an interglacial time scale of 130,000 years, northern peatlands have always in warmer periods accumulated significant quantities of C<sup>3</sup>. In contrast to such steady C accumulation over long time scales, the processes and mechanisms that govern C fluxes and accumulation over short time scales are complex and often difficult to predict<sup>4,5</sup>. Also, as the mean annual rate of soil C accumulation is low<sup>6</sup>, a sudden switch from a C sink to a C source can take place under changing environmental conditions either at a scale of microsites<sup>7,8</sup> or entire peatlands<sup>9,10</sup>. Such short-term dynamics complicate the prediction and modelling of peatland C fluxes, including the responses of fluxes to the climate change, by leading to a signal-to-noise problem, where it is difficult to determine if short-term observations represent long-term trends or are simply short-term “noise”.

<sup>1</sup>Natural Resources Institute Finland (Luke), Latokartanonkaari 9, Helsinki 00790, Finland. <sup>2</sup>Ecosystems and Environment Research Programme, Faculty of Biological and Environmental Sciences, University of Helsinki, Niemenkatu 73, Lahti 15140, Finland. <sup>3</sup>Climate System Research, Finnish Meteorological Institute, Erik Palménin aukio 1, Helsinki 00560, Finland. <sup>4</sup>Natural Resources Institute Finland (Luke), Paavo Havaksen tie 3, Oulu 00790, Finland. <sup>5</sup>Geography Research Unit, Faculty of Science, University of Oulu, Pentti Kaiteeran katu 1, Oulu 90570, Finland. <sup>6</sup>Ecosystems and Environment Research Programme, Faculty of Biological and Environmental Sciences, University of Helsinki, Viikinkaari 1, Helsinki 00790, Finland. ✉email: juha.mikola@luke.fi

At short time scales, C cycling in peatlands is controlled by surface microtopography<sup>7</sup>, which creates variation in plant species composition, plant growth and oxidation of CH<sub>4</sub> emissions<sup>8,11–14</sup>, and soil fertility<sup>15</sup>, which limits primary production. Of these two drivers, surface microtopography and its consequences are well established: peatlands are commonly fragmented into meter-scale wet depressions called flarks or hollows and dry mounds called strings or hummocks<sup>5</sup>, and while strings have a relatively thick (20–50 cm) soil layer above the water table (WT), thus enabling oxidation of CH<sub>4</sub> produced in deeper soil layers, soil surface in flarks is at or below the WT. Between these, lawns can be defined as surfaces that are above the WT, but still distinctly lower than strings. The microforms are known to have contrasting plant community structure and production<sup>11–13</sup>, different litter decomposition rate<sup>16</sup> and different relative contribution of methanogenesis to soil C emissions<sup>8</sup>, which eventually leads to differences in the quantity and form of C fluxes<sup>7,8,14</sup>. In terms of ecosystem functioning, strings typically have higher gross primary production (GPP) and higher ecosystem respiration (R<sub>e</sub>) than flarks<sup>8,13,15</sup>, while flarks release a bigger proportion of soil C emissions as CH<sub>4</sub><sup>8,14</sup>.

In contrast to the comprehensive understanding of the role of microtopography, the understanding of how nutrient variation controls biogeochemical cycling and gas exchange across peatlands seems to lack clarity. For instance, the influence of soil fertility (the capacity to support net primary production, NPP) on peatland C cycling is often perceived through the bog-fen gradient: bogs (typically dominated by *Sphagnum* mosses and woody plants) rely on nutrients in rainwater and are supposed to be less fertile than fens (characterized by graminoids), which receive nutrients from groundwater or surface water input. However, the bog-fen gradient is poorly associated with NPP, mostly due to some fens being very unproductive<sup>17</sup>, and while some studies have found that plant production and net ecosystem exchange (NEE) of CO<sub>2</sub> are lower on bog sites than fen sites<sup>15</sup>, bogs can also locally sustain higher<sup>18</sup> or similar<sup>19</sup> NPP than fens. Other attributes of C cycling seem to better obey the bog-fen gradient though: CH<sub>4</sub> fluxes are lower in bogs, especially in boreal and subarctic areas<sup>20</sup> and bogs have on average higher rate of C accumulation than fens<sup>6,21,22</sup>. Besides the bog-fen gradient, soil fertility differs between fen complexes, and due to the inflow of water into fens, within fens<sup>23,24</sup>. Not much is known of the influence of this variation, but experiments have shown that *Carex* growth increases with increasing N supply across those fertility gradients that are found among natural fens<sup>25,26</sup>. It also appears that the potentially peat forming production of *Carex* roots increases with increasing N availability<sup>26</sup>, and that CH<sub>4</sub> emissions are greater in rich than poor fens, where substrate availability limits CH<sub>4</sub> production<sup>27</sup>. All in all, despite the extensive literature available on peatland C cycling, the importance of nutrient variation in controlling C cycling is poorly understood.

To address the gap in knowledge, we (1) examined the relative effects of fertility variation and microtopography on CO<sub>2</sub> and CH<sub>4</sub> exchange within a northern boreal fen ecosystem. Using plant and soil samples collected across the fen we analysed (2) how these effects were linked to variation in plant and soil attributes and decomposition rate of plant litter. To study (3) how temperature and WTL affect CO<sub>2</sub> and CH<sub>4</sub> exchange, and especially if they can modify the microtopography and fertility effects, we examined gas exchange data collected during three growing seasons of different air temperature and precipitation. Finally, to contribute to the recent literature about the effects of *Sphagnum* lawn expansion in northern fens under climate change<sup>22,28</sup>, we (4) compared data of plant and soil parameters in lawns extensively and partly covered by *Sphagnum* mosses. We used moss species as indicator plants for soil nutrient availability<sup>29,30</sup> to define fertility zones within the fen, and collected gas exchange data by eddy covariance (EC) and static chamber methods to examine C flux dynamics at both ecosystem, and microform and fertility zone scales.

## Materials and methods

### Field site and land cover types

A micrometeorological flux station was established on Halssiaapa, a boreal peatland<sup>31</sup>, in Sodankylä, northern Finland (67.36850 °N, 26.65456 °E; 180 m a.s.l.) in 2012 to provide EC measurements of the ecosystem–atmosphere exchange of CO<sub>2</sub> and CH<sub>4</sub> (the setup of the EC tower is described in more detail later in the text). Around the EC tower, the landscape has a typical aapa mire microtopography with low strings, lawns and flarks, and a 0.2° upward slope towards north-east (Figs. 1 and 2, Supplementary Table 1). Nearest Scots pine (*Pinus sylvestris* (L.)) forest is ca. 230 m from the tower (Fig. 1). During reference years 1991–2020, the mean annual temperature in the area was 0.3 °C, the precipitation was 543 mm and the mean air temperatures of January and July were –12.5 and 15.0 °C, respectively<sup>32</sup>.

In a field survey in 2014, four main land cover types (LCTs) were distinguished around the EC tower using ground-based visual judgement (Supplementary Table 1). These LCTs were flark (high WTL with patches of open water and peat, graminoids dominating vascular plants), lawn (intermediate WTL with graminoids, shrubs and mosses dominating vegetation), string (low WTL with trees, shrubs and mosses dominating vegetation) and forest (*P. sylvestris* canopy cover ≥ 10%). The lawn was further split into lawn and *Sphagnum* lawn, the latter being characterized by almost continuous *Sphagnum* cover (Fig. 2). The string was split into birch string (trees mostly *Betula pubescens* (Ehrh.)) and pine string (trees mostly *P. sylvestris*) (Supplementary Table 1). A tiny proportion of the study area is covered by boardwalks and the instrument shed. The methods used for the land cover classification in the land cover map (Fig. 1) are described in Supplementary Text 1 and Supplementary Table 3, and the magnitude of the WTL difference among the microforms is shown in Fig. 3b.

### Study plots, and vegetation and soil measurements

To characterize the vegetation and soil properties in the area, study plots were established in early summer 2014 along 16 compass points at regular distances of 25, 50, 75, 100, 150 and 250 m from the EC tower (Fig. 1). Of these, 48 plots were in 2014 selected for soil and plant analyses in a way that covered the main area of measurements near the EC tower but also provided a sufficiently balanced set of plots from string, lawn, *Sphagnum* lawn and flark (Fig. 1, Supplementary Table 2).

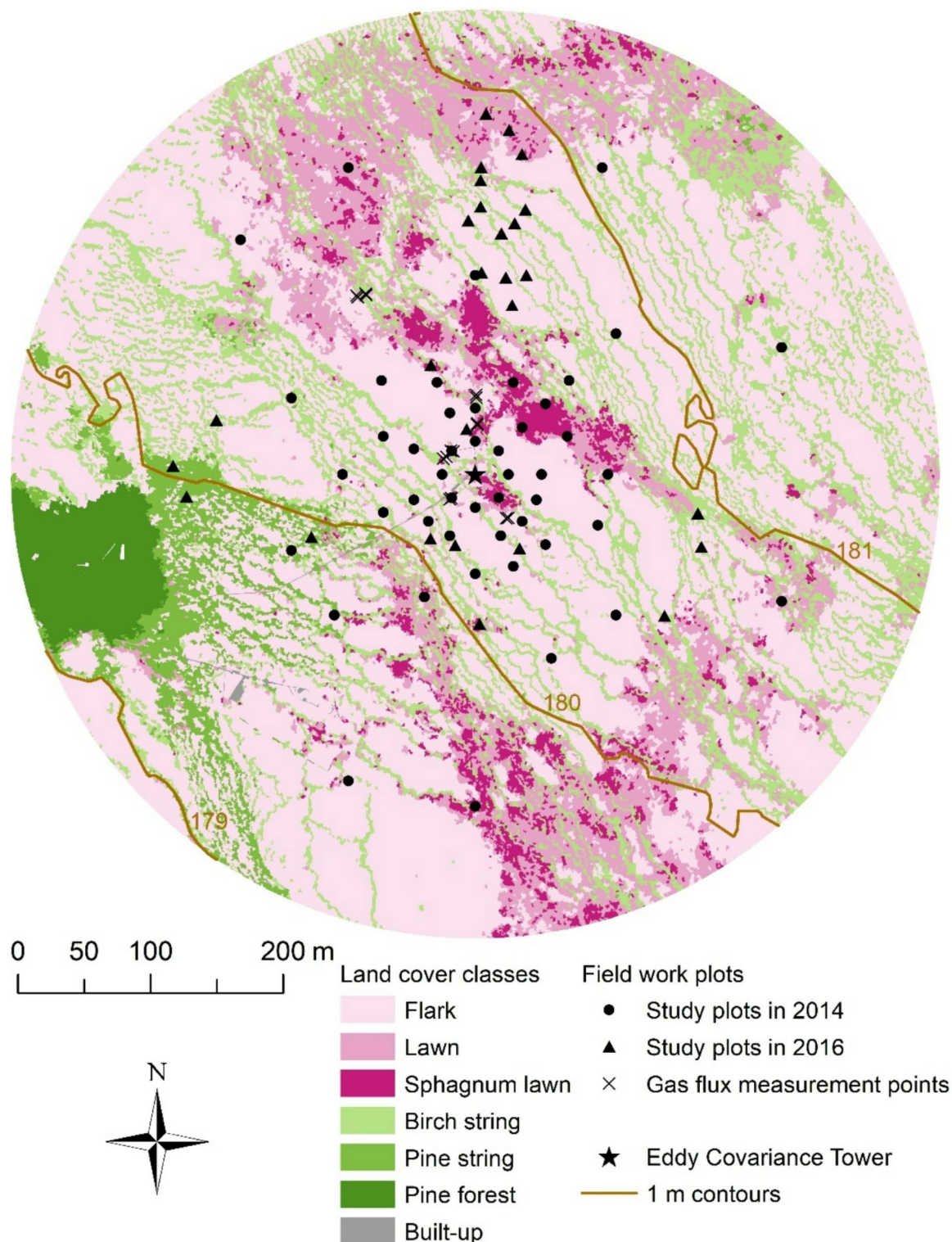


**Fig. 1.** Land cover classification, contour lines and location of field work plots in the study area at Halssiaapa, Sodankylä, Finland (67.36850 °N, 26.65456 °E; 180 m a.s.l.). The method used for generating the land cover classification is provided in the Supplementary Text 1.

In addition to being classified in terms of microform, each plot was also classified either as eutrophic, mesotrophic or oligotrophic based on the species composition of mosses in the ground layer. Nutrient demanding brown moss species, such as *Hamatocaulis vernicosus* ((Mitt.) Hedenäs), *Tomentypnum nitens* ((Hedw.) Loeske), *Campylium stellatum* ((Hedw.) Lange & C.E.O.Jensen), *Helodium blandowii* ((F.Weber & D.Mohr) Warnst.) and *Dicranum bonjeanii* (De Not) were considered as a sign of eutrophic conditions. Mesotrophic conditions



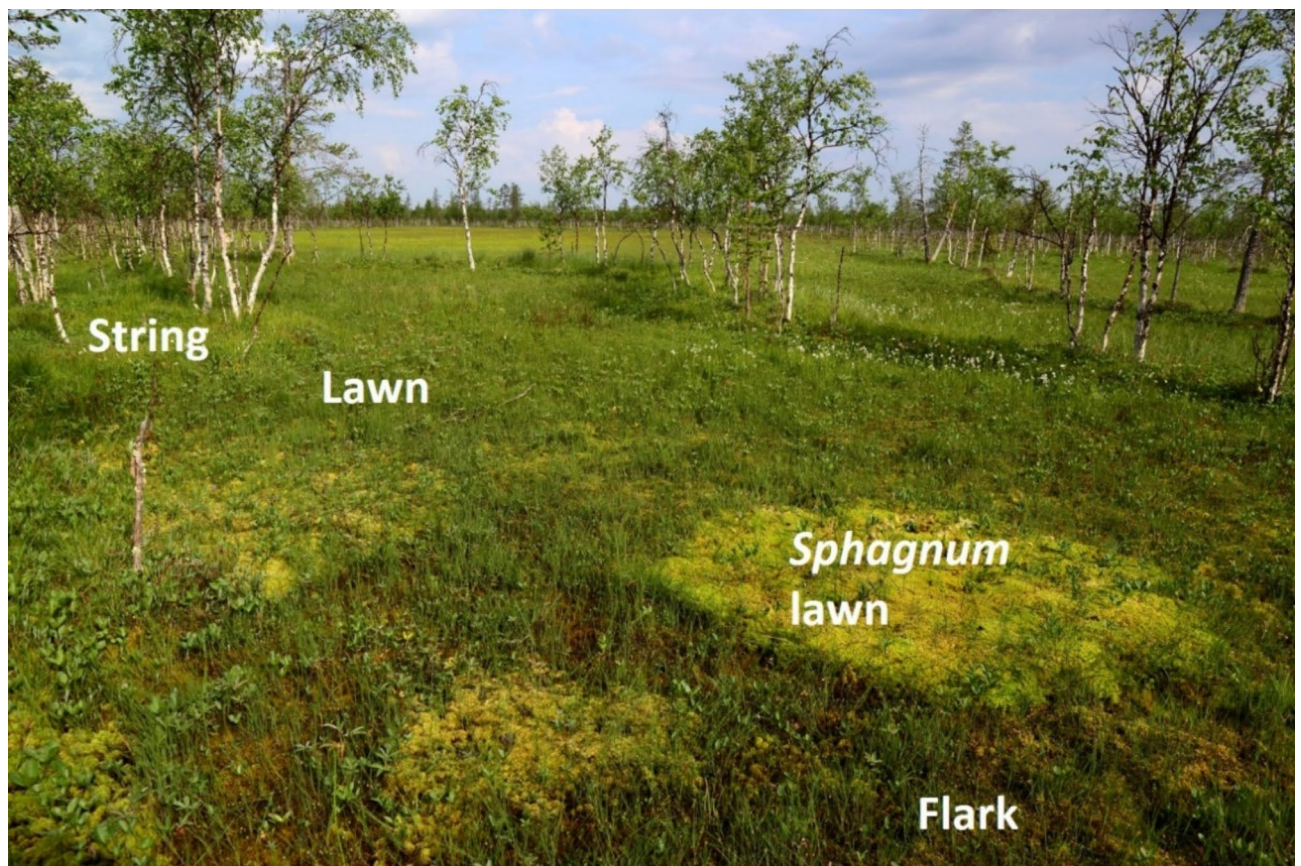


**Fig. 2.** A picture illustrating the string, lawn, *Sphagnum* lawn and flark microforms of Halssiaapa fen.

were assumed to have no eutrophic species but moderately nutrient demanding species, such as *Sphagnum teres* ((Schimp.) Ångstr.), *S. warnstorffii* (Russow), *S. subsecundum* (Nees), *S. riparium* (Ångstr.) or *Sarmentypnum exannulatum* ((Shimp.) Hedenäs). Finally, oligotrophic conditions were assumed to have no eutrophic or mesotrophic species but species requiring minerotrophy, such as *S. lindbergii* (Schimp.), *S. balticum* (Russow), *S. papillosum* (H.Lindb.) or *S. fallax* (H. Klinggr.). For the ecological niches of the moss species we relied on descriptions in Euroala et al.<sup>29</sup> and Laine et al.<sup>30</sup>.

For each study plot, three subplots (50 cm × 50 cm) were established 2 m from the plot midpoint to compass directions E, N and W. Plant species were identified, and the areal cover of abundant species and plant functional groups were estimated for each subplot on 17th–19th of July 2014, at the moment of assumed maximum plant biomass. One of the subplots was then destructively harvested (excluding trees) to estimate plant aboveground biomass and single-sided vascular plant leaf area index (LAI, m<sup>2</sup> leaf m<sup>-2</sup> ground). As in earlier studies for northern peatland ecosystems<sup>33</sup>, for biomass estimates, the ground and field layer plants were classified into six functional groups following Chapin III et al.<sup>34</sup>: (1) *Sphagnum* mosses, (2) other mosses, (3) dwarf shrubs, (4) *Betula nana* (L.), (5) forbs and (6) graminoids (*Carex* and *Scheuchzeria palustris* (L.)). To estimate the biomass of (7) deciduous trees (*B. pubescens*) and (8) evergreen trees (*P. sylvestris*), the diameter of stems (at 1.3 m) of trees growing within a larger circular area (diameter 10 m) was measured. The aboveground biomass of *B. pubescens* was estimated using linear regressions of stem diameter and biomass given in Starr et al.<sup>35</sup>. For *P. sylvestris*, stem volume was first calculated using the models given in Varmola and Vuokila<sup>36</sup> for “small-sized pines” and the stem, branch and foliage biomass were then estimated following the procedure in Kauppi et al.<sup>37</sup>.

To estimate the ability of microbes to decompose standard plant litter on the soil surface and deeper in the peat, one teabag (2 g dry mass of Lipton® Pyramid green tea<sup>38</sup>) and one litter bag filled with oat, *Avena sativa* (L.) straw (3 g dry mass) were placed on the ground and buried at the depth of 10 cm near each harvested subplot on 8th of June 2014. All bags were collected after seven and half weeks of litter decomposition (on 19th and 20th of August), and the tea and straw were dried (70 °C, 48 h) to estimate litter mass loss.

Soil samples were collected in mid-July 2014 from the 48 harvested subplots. At each plot, a sample of approximately 5 cm × 5 cm × 5 cm was cut out of the soil at 0–5 cm depth (straight under the green parts of the moss, i.e. this layer also includes moss and other plant litter) and at 15–20 cm depth. The samples were dried (70 °C, 48 h) for bulk density estimates and later ground in a ball mill to measure their C and N concentrations using a CNS-2000 analyser (LECO Corporation, Saint Joseph, MI, USA). Sample C and N content (g dm<sup>-3</sup>) were then calculated using the bulk density and C and N concentrations. The pH was measured in the field for each plot using a sample of water taken from the bottom of a 30 cm deep hole. Soil measurements carried out in 2014

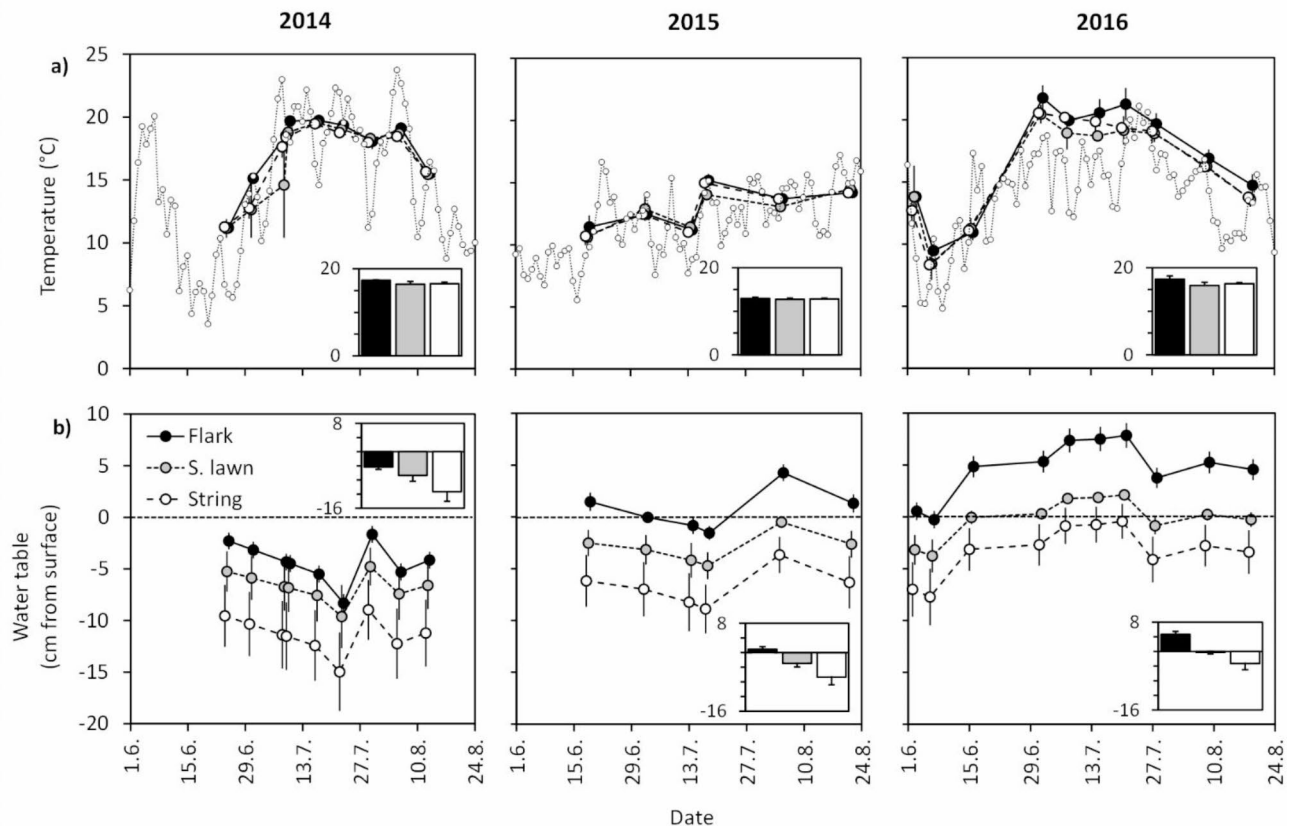


**Fig. 3.** Mean (a) daily air temperature (dashed line with tiny symbols) and daytime soil temperature (10 cm depth), and (b) water table level in boreal fen microforms (S. lawn = *Sphagnum* lawn) in summers 2014–2016 ( $\pm$  SE;  $n = 3$  for flark and string,  $n = 2$  for *Sphagnum* lawn). Bars in insets show growing season mean values ( $\pm$  SE;  $n$  as for daily measures).

were supplemented in 2016 with another set of 23 randomly assigned plots (Fig. 1) to better cover the different microforms and eutrophic zones (Supplementary Table 2).

### Chamber measurements of CO<sub>2</sub> and CH<sub>4</sub> fluxes

Ecosystem exchange of CO<sub>2</sub> and CH<sub>4</sub> in different microforms and fertility zones was quantified using the static chamber method. Permanent aluminium collars (60 cm  $\times$  60 cm), with sleeves extending to 30 cm below the soil surface, were assembled on string ( $n = 6$ ), *Sphagnum* lawn ( $n = 4$ ) and flark ( $n = 6$ ) microforms in the central parts of the study area (Fig. 1) after soil thaw and two weeks before starting the measurements in 2014.

The CO<sub>2</sub> and CH<sub>4</sub> fluxes were quantified during one-day measurement rounds weekly or every other week (depending on weather conditions and staff availability) from 17th of June to 12th of August in 2014, from 17th of June to 27th of August in 2015, and from 2nd of June to 24th of August in 2016. All measurement rounds were carried out in daytime (8 a.m.–7 p.m.). Individual rounds were performed for CO<sub>2</sub> and CH<sub>4</sub>, with one flux measurement for each field point at each round. The order of field points was varied among the measurement rounds to avoid the time of the day confounding the microform and fertility zone mean effects. During the study, the vegetation, peat or WT did not show signs of disturbance inside or next to the collars.

During measurements, the chamber (height 32 cm) was placed air-tightly on the water-filled groove of the collar and the chamber air temperature and soil temperature (PT100 sensor, Gräff GmbH, Germany) and WTL (cm from soil surface) were recorded. WTL was measured manually from vertical plastic tubes, permanently installed in the soil beside every collar. String and flark collars were evenly distributed among eutrophic, mesotrophic and oligotrophic zones (two collars for both microforms at each fertility zone), while all four *Sphagnum* lawn collars were at the mesotrophic zone (Supplementary Table 2). Therefore, to not confound microform and fertility zone effects, only string and flark measurements are included when assessing fertility effects on GHG fluxes. All collars were used for measuring CH<sub>4</sub> fluxes, half of the collars for measuring CO<sub>2</sub> fluxes (Supplementary Table 2).

An opaque chamber was used to measure CH<sub>4</sub> exchange. During the 20-min chamber closure, four samples of air were collected from the chamber headspace using a syringe 5, 10, 15 and 20 min after the chamber was placed on the collar. Samples were stored in 12 ml gas-tight Labco Exetainer® glass vials (Labco Limited, Lampeter, UK) and analysed in a Natural Resources Institute Finland (Luke) laboratory using a gas chromatograph (Agilent



7890 A, Agilent Technologies, U.S.A.), equipped with a FI-detector and a 2-m long HayeSep Q Packed GC Column (80/100 mesh, 2 mm ID).

To measure the net ecosystem exchange (NEE) of CO<sub>2</sub>, a transparent plexiglass chamber was used. The chamber was equipped with a fan and a self-constructed thermostatic cooling system that maintained the chamber air temperature within  $\pm 2$  °C of ambient. During the 2-min chamber closure, air CO<sub>2</sub> concentration was monitored using an infrared gas analyser (EGM 4, PP-systems) and the photosynthetically photon flux density (PPFD) was measured within the chamber using a high-quality sensor (PQS1 PAR Quantum Sensor, Kipp&Zonen, or similar). To obtain measurements under different PPFD levels, the NEE measurement under natural irradiation conditions was followed by measurements under 65% and 88% reduced irradiation (except when the level of full light was already low, only 65% reduction was applied). The reduction was achieved using shading nets placed over the chamber. Ecosystem respiration ( $R_e$ ) was measured in the dark using an opaque hood placed over the chamber. After each closure, the chamber was properly vented. The chamber volume was corrected for ground surface variation by measuring the true difference between ground surface and chamber top for each collar individually. Notably, the chamber measurements only included the CO<sub>2</sub> exchange of ground vegetation, and not that of trees, as any existing *B. pubescens* and *P. sylvestris* roots were disconnected when the collars were installed into the soil.

### Calculation of chamber fluxes

All chamber data were first checked, based on expert judgement of starting values and pattern of temporal changes during measurements, to remove cases of abnormally high starting concentrations, leak, saturation or disturbance-induced ebullition. Flux rates of CO<sub>2</sub> and CH<sub>4</sub> were then calculated using linear regressions, taking into account the chamber volume, air pressure and air temperature. That our data only include diffusive CH<sub>4</sub> flux and not ebullition should not affect the microform and fertility zone comparisons of CH<sub>4</sub> exchange but may underestimate the overall net CH<sub>4</sub> emission.

For CO<sub>2</sub>, one transparent chamber closure provided the CO<sub>2</sub> flux or NEE for the recorded PPFD level. Using  $R_e$ , the gross primary production (GPP) was calculated as:

$$\text{GPP} = \text{NEE} - R_e \quad (1)$$

To be able to compare the GPP and NEE values obtained in varying light conditions, the data were standardised, following Heiskanen et al. (2021)<sup>8</sup> and Silfver et al. (2020)<sup>39</sup>, to a common irradiation level of 1200  $\mu\text{mol m}^{-2} \text{s}^{-1}$ , which represents near-optimal photosynthetic conditions in the region<sup>40</sup>. In brief, the GPP rates were first parameterised for each plot and measurement day by utilising the empirical light-response of photosynthesis<sup>41</sup>:

$$\text{GPP} = \frac{\text{PPFD} \times \alpha \times \text{GP}_{\max}}{\text{PPFD} \times \alpha + \text{GP}_{\max}} \quad (2)$$

where PPFD is the measured photosynthetic photon flux density during the closure,  $\alpha$  is the initial slope between GPP and PPFD, and  $\text{GP}_{\max}$  is the theoretical maximum gross photosynthesis rate.

The fitting of Eq. 2 requires GPP values from a wide irradiation range to provide robust results. Due to a lack of different light levels on some days, a time-invariant parameter  $k = \alpha / \text{GP}_{\max}$  was determined for each microform (Supplementary Table 4). The microform-specific  $k$  was calculated from the fitted  $\alpha$  and  $\text{GP}_{\max}$  values as a variance-weighted mean, discarding the fits of days which had a relative error greater than 100%. Fixing the  $\alpha / \text{GP}_{\max}$  ratio has been shown to markedly decrease the uncertainty of GPP parameterisation<sup>8</sup>. The day-specific GPP<sub>1200</sub> values were then calculated for each plot by fitting the data to modified Eq. 2 with fixed  $k$  and free  $\text{GP}_{\max}$  parameters. The NEE<sub>1200</sub> values were estimated using Eq. 1 and daily average  $R_e$  values<sup>8,39</sup>.

### Eddy covariance estimates of CO<sub>2</sub> and CH<sub>4</sub> exchange

In addition to the instantaneous chamber estimates, the GHG exchange between the atmosphere and the fen has been quantified since 2013 using the micrometeorological eddy covariance (EC) method, which provides continuous, ecosystem-scale exchange data. In this study, we utilized the EC data collected simultaneously with the chamber measurements during the growing seasons 2014–2016. The EC measurements were conducted on a tower 7 m above the mean fen surface. The EC system consisted of a three-dimensional anemometer (USA-1, METEK Meteorologische Messtechnik GmbH, Germany), a closed-path infrared gas analyser for CO<sub>2</sub> and H<sub>2</sub>O mixing ratios (LI-7000, LI-COR Biosciences, USA) and a laser-based gas analyser for CH<sub>4</sub> mixing ratio (RMT-200, Los Gatos Research, USA). The EC data were sampled at 10 Hz, and standard methods were used to calculate half-hourly turbulent fluxes<sup>42</sup>. Further details on the data processing protocol are provided by Aurela et al. (2009)<sup>43</sup>.

The total net ecosystem exchange (NEE) measured by EC was partitioned into two main components: ecosystem respiration ( $R_e$ ) and gross primary production (GPP). This partitioning was achieved by using a simple temperature response for respiration and a radiation response for GPP<sup>43</sup>. The footprint climatology of the EC-based fluxes is not considered in this study and the fluxes are not directly comparable to those derived from chamber measurements, but rather provide an estimate of the seasonal cycle and enhance the understanding of the ecosystem-scale GHG exchange patterns.

### Temperature and water table level

To compare the years 2014–2016 in terms of environmental conditions, the start and end of the growing season were first determined. The growing season was considered to start when five days in row had mean air temperature  $> 5$  °C and to end when five days in row had mean temperature  $< 5$  °C. Heat sum (expressed as

degree days, DD) was then calculated for each growing season using 5 °C as a threshold. Air temperature was measured at 3 m using a HMP155 probe (Vaisala Oyj, Finland). Soil temperature and WTL were measured at each GHG chamber measurement, being thus available for different microforms from the beginning of June to the end of August for each year. Soil temperature was measured using a hand-held PT100 sensor (Gräff GmbH, Germany), and in this study, measurements at 10 cm depth are used to illustrate soil temperature variation.

### Statistical analysis

To estimate the quantity of variation explained by microform and fertility zone in GHG exchange data, variance components were calculated using the SPSS general linear model (GLM) variance components procedure. Year was added into the calculation model as a fixed factor, and when calculating the variance component for fertility zone, *Sphagnum* lawn (which only had mesotrophic plots) was excluded from the data. The residuals of GHG exchange data were normally distributed and the data needed no transformation. The statistical significance of microform and fertility zone effects on GHG exchange was not tested because the low number of replicates ( $n=2-3$  for CO<sub>2</sub> exchange and 2015 CH<sub>4</sub> exchange,  $n=4-6$  for 2014 and 2016 CH<sub>4</sub> exchange; Supplementary Table 2) does not allow powerful tests and creates an excessive risk of Type II error (accepting the null hypothesis when it is false). For the same reason, microform effects on soil temperature and WTL, which were recorded along with GHG chamber measurements, were not statistically tested.

The effects of microform and fertility zone on vegetation variables (*Sphagnum*, other moss, total moss, dwarf shrub, forb, graminoid, total vascular plant and total plant dry mass, ground layer vascular plant LAI), soil variables (water content, bulk density, C and N concentration, and C and N content in the 0–5 cm and 15–20 cm soil layers) and litter decomposition (tea and straw mass loss on the ground and at the depth of 10 cm) were tested using multivariate analysis of variance (MANOVA) models (with no interaction effect included) and the statistically significant differences between microform and fertility zone means were revealed using Student-Newman-Keuls (SNK) post-hoc tests. As four *Sphagnum* lawn plots had no fertility classification in soil data (Supplementary Table 2), the models were run twice for soil variables: first with these plots included (testing microform effect) and then with these plots excluded (testing fertility zone effect). To achieve normal distribution of residual variation, all soil parameters were log<sub>10</sub>-transformed. Of the plant parameters, total moss dry mass and ground layer vascular plant LAI were square root-transformed and the dry mass of *Sphagnum* mosses, dwarf shrubs, forbs, all vascular plants, and all plants were log<sub>10</sub>-transformed. Correlation of variables within and between soil layers as well as between plant and soil variables were tested using Pearson's correlation test.

## Results

### Environmental attributes

The growing season lasted for 127 days in 2014 (17th of May–20th of September), 136 days in 2015 (19th of May–1st of October) and 165 days in 2016 (27th of April–8th of October). The growing season temperature sum was 20% lower in 2015 (813 DD with a 5 °C threshold) than in 2014 (1014 DD) and 2016 (1026 DD) and the June–August period was on average 2 °C colder in 2015 (mean air temperature 11.8 °C) than in 2014 (14.0 °C) and 2016 (13.5 °C) (Fig. 3a). Temporal variation in soil temperatures (10 cm depth) closely mirrored the seasonal development of air temperatures except in the first half of July 2016 when soil temperatures were slightly higher than air temperatures (Fig. 3a). On average, soil temperatures were almost 4 °C lower in 2015 (mean 12.9 °C over all microforms and measurements) than in 2014 (16.8 °C) and 2016 (16.5 °C) (Fig. 3a). The precipitation during the May–August period was lowest in 2014 (247 mm), intermediate in 2015 (316 mm) and highest in 2016 (327 mm) (Supplementary Fig. 1). WTL followed the trend in precipitation: it was on average lowest in 2014 (7.5 cm below surface when calculated over all microforms and measurements), intermediate in 2015 (2.9 cm below surface) and highest in 2016 (0.4 cm above surface) (Fig. 3b).

Flark had ca. 1.0 °C higher mean daytime soil temperature than *Sphagnum* lawn and string in the 2014 and 2016 growing seasons, while in the 2015 growing season, this difference was only 0.2 °C (Fig. 3a). Differences in WTL among the microforms were clear but varied slightly among the years: e.g. the difference was 2.5 cm for flark and *Sphagnum* lawn in 2014 and 5 cm in 2016 (Fig. 3b).

### CO<sub>2</sub> exchange

In chamber measurements, the NEE<sub>1200</sub> was constantly negative, meaning that all microforms and fertility zones were CO<sub>2</sub> sinks at optimal irradiation conditions throughout the growing seasons (Fig. 4a, b). Based on the variance component calculation, microform explained 36% and 39% and fertility 10% and 12% of total NEE<sub>1200</sub> and GPP<sub>1200</sub> variation, respectively (Fig. 4a–d). String had on average 144% higher NEE<sub>1200</sub> and 141% higher GPP<sub>1200</sub> than flark and *Sphagnum* lawn (Fig. 4a, c), while the eutrophic and mesotrophic zones had on average 111% higher NEE<sub>1200</sub> and 102% higher GPP<sub>1200</sub> than the oligotrophic zone (Fig. 4b, d). Microform explained 31% and fertility 15% of total ecosystem respiration, R<sub>e</sub> variation (Fig. 4e, f). String had on average 85% higher R<sub>e</sub> than flark and *Sphagnum* lawn (Fig. 4e), and the eutrophic and mesotrophic zones 83% higher R<sub>e</sub> than the oligotrophic zone (Fig. 4f).

When EC estimates of NEE<sub>1200</sub>, GPP<sub>1200</sub> and R<sub>e</sub> were averaged across all June–August EC values (Table 1), years 2014 and 2016 differed from the year 2015: GPP<sub>1200</sub> was 24% higher in 2014 and 2016 than in 2015; R<sub>e</sub> was 33% and 21% higher in 2014 and 2016, respectively, than in 2015; and finally, NEE<sub>1200</sub> was 20% and 27% higher in 2014 and 2016, respectively, than in 2015 (Fig. 4).

### CH<sub>4</sub> exchange

In daytime chamber measurements, all microforms and fertility zones were constant CH<sub>4</sub> emitters (Fig. 5a, b). Based on the variance component calculation, microform explained 14% and fertility 36% of total CH<sub>4</sub> flux

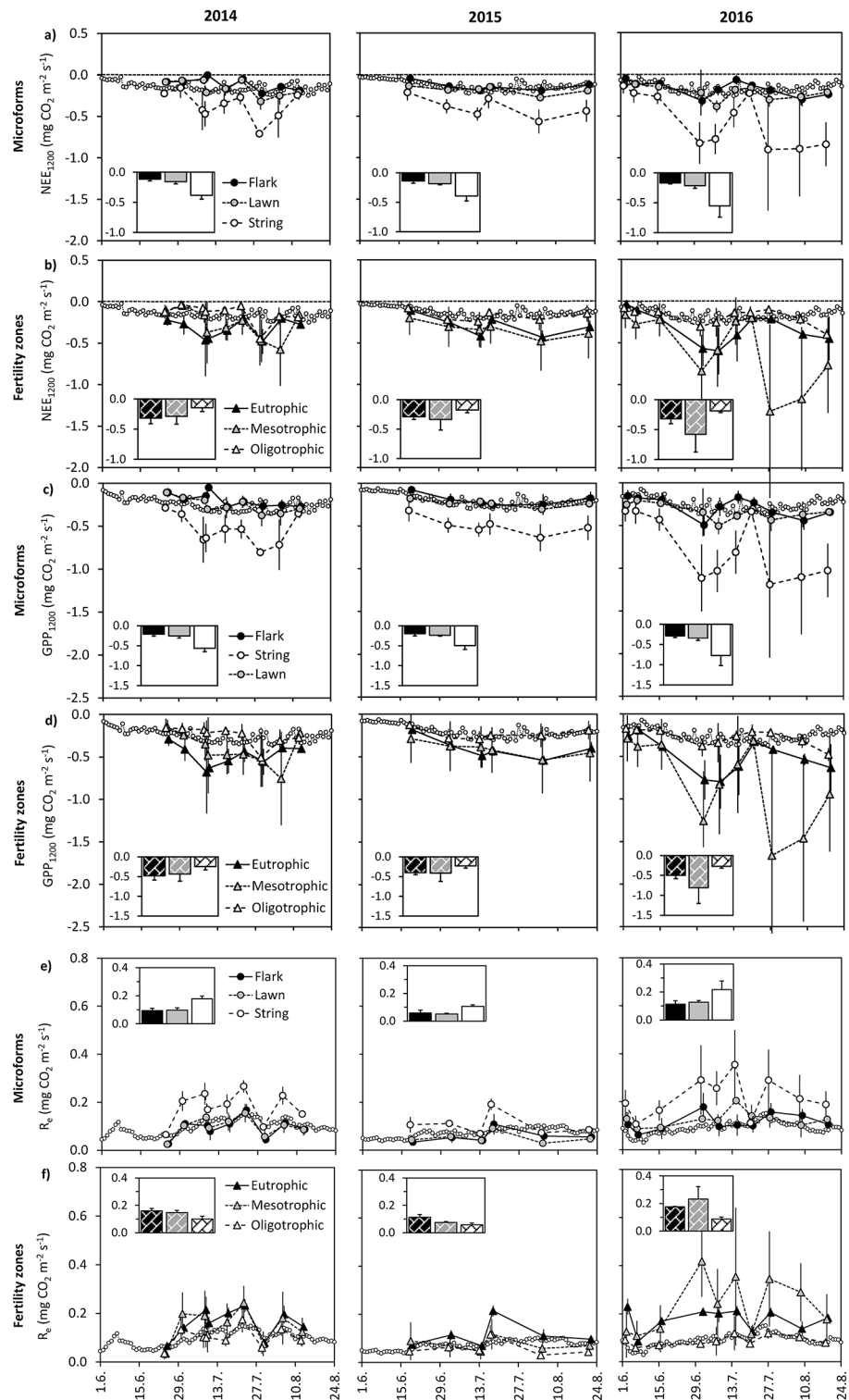


**Fig. 4.** Daytime (a, b)  $\text{CO}_2$  exchange, i.e. potential net ecosystem exchange  $\text{NEE}_{1200}$ , (c, d) potential gross primary production  $\text{GPP}_{1200}$  and (e, f) ecosystem respiration  $R_e$ , measured using static chambers for boreal fen microforms (S. lawn = *Sphagnum* lawn) and fertility zones in summers 2014–2016 (mean  $\pm$  SE;  $n = 3$  for flark and string,  $n = 2$  for *Sphagnum* lawn,  $n = 2$  for all fertility zones). The bars in insets (even surface for microforms, bricks for fertility zones) show June–August mean flux ( $\pm$  SE;  $n$  as for daily fluxes) and the tiny symbols give ecosystem scale daily daytime (9 a.m.–4 p.m.) means of  $\text{CO}_2$  exchange, measured using the EC method and not standardized to irradiation level of  $1200 \mu\text{mol m}^{-2} \text{s}^{-1}$ .



	2014	2015	2016
GPP <sub>1200</sub> (mg CO <sub>2</sub> m <sup>-2</sup> s <sup>-1</sup> )	-0.245	-0.197	-0.245
R <sub>e</sub> (mg CO <sub>2</sub> m <sup>-2</sup> s <sup>-1</sup> )	0.097	0.073	0.088
NEE <sub>1200</sub> (mg CO <sub>2</sub> m <sup>-2</sup> s <sup>-1</sup> )	-0.149	-0.124	-0.157
CH <sub>4</sub> (μg m <sup>-2</sup> s <sup>-1</sup> )	1.31	0.78	1.90

**Table 1.** Mean June–August ecosystem scale NEE<sub>1200</sub>, GPP<sub>1200</sub>, R<sub>e</sub> and CH<sub>4</sub> exchange for study years 2014–2016, as quantified using the eddy covariance method. Daily estimates are shown in Figs. 3 and 4

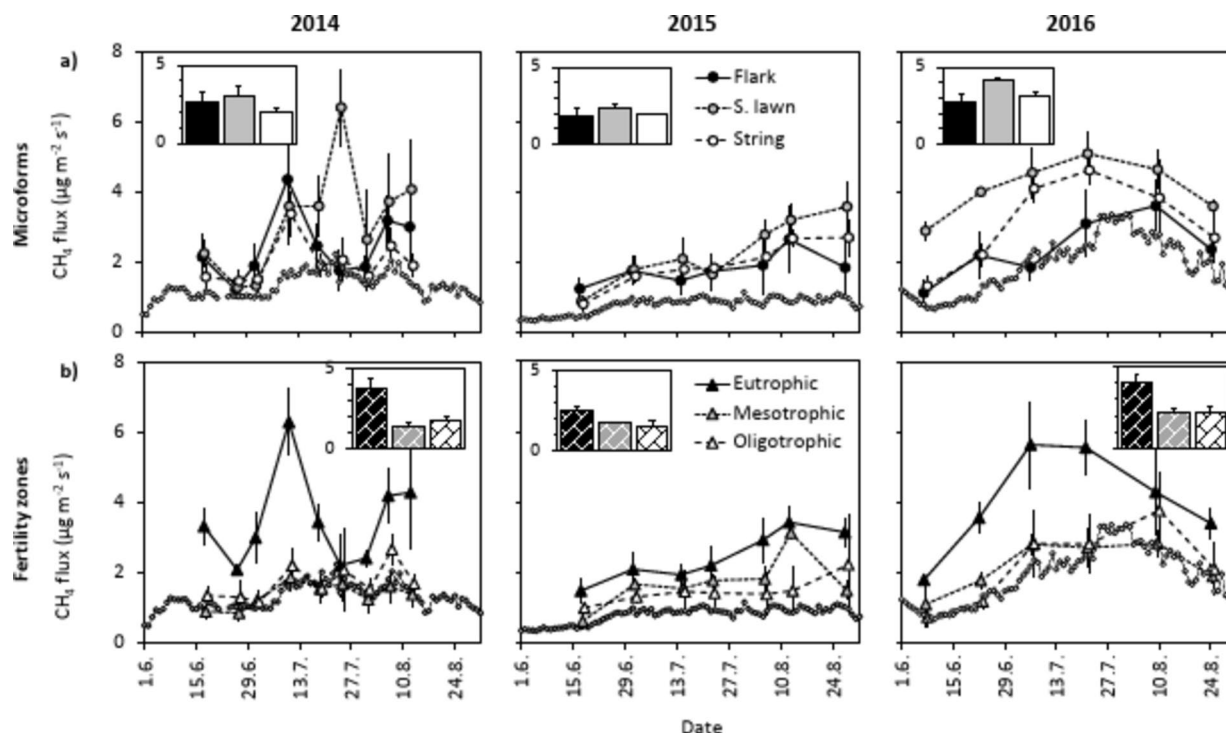


**Fig. 5.** Daytime CH<sub>4</sub> exchange in boreal fen (a) microforms (*S. lawn* = *Sphagnum* lawn) and (b) fertility zones in summers 2014–2016 ( $\pm$  SE;  $n=3$ –6 for flark and string,  $n=2$ –4 for *Sphagnum* lawn,  $n=2$ –4 for all fertility zones). The bars in insets (even surface for microforms, bricks for fertility zones) show June–August mean daytime flux ( $\pm$  SE;  $n$  as for daily fluxes) and the tiny symbols show mean daily ecosystem-scale CH<sub>4</sub> exchange, measured using the EC method.

variation (Fig. 5a, b). *Sphagnum* lawn had on average 35% higher emissions than flark and string, but this difference also varied among the years, being 34% in 2014, 22% in 2015 and 45% in 2016 (Fig. 5a). The eutrophic zone had on average 93% higher CH<sub>4</sub> emissions than the mesotrophic and oligotrophic zones, but also this difference varied among the years, being 145% in 2014, 55% in 2015 and 84% in 2016 (Fig. 5b).

The mean EC estimates across June–August (Table 1) show that CH<sub>4</sub> emissions were 144% and 68% higher in 2016 and 2014, respectively, than in 2015 (Fig. 5).

### Plant biomass and vascular plant LAI

For plant variables (Fig. 6), the MANOVA multivariate statistics (Wilks' lambda) showed a highly significant microform effect ( $P < 0.001$ ; see complete statistics in Supplementary Table 5). Of the plant functional groups, *Sphagnum* and other mosses had a contrasting pattern: *Sphagnum* mosses were abundant in string and *Sphagnum* lawn and mostly absent in lawn and flark ( $P < 0.001$ ), which in turn were the main sites for other mosses ( $P = 0.017$ ) (Fig. 6). Due to a such complementary pattern, total moss mass did not significantly differ among the microforms ( $P = 0.199$ ) (Fig. 6).

*Betula pubescens* and *P. sylvestris* trees were exclusively found in string (Fig. 6). The mean biomass of *B. pubescens* was five-fold in comparison to *P. sylvestris*. *Betula nana* was most abundant in string, but also had a low biomass in lawn (Fig. 6). Dwarf shrub biomass was lower in flark than in other microforms ( $P < 0.001$ ) (Fig. 6). Forbs had significantly higher biomass in string and *Sphagnum* lawn than in lawn and flark ( $P < 0.001$ ), whereas graminoids did not statistically significantly differ among the microforms ( $P = 0.236$ ) (Fig. 6). Mostly due to the distribution of woody species, total vascular plant mass was higher in string than other microforms ( $P < 0.001$ ) (Fig. 6). Total plant mass (sum of moss and vascular plant mass) was also significantly higher in string

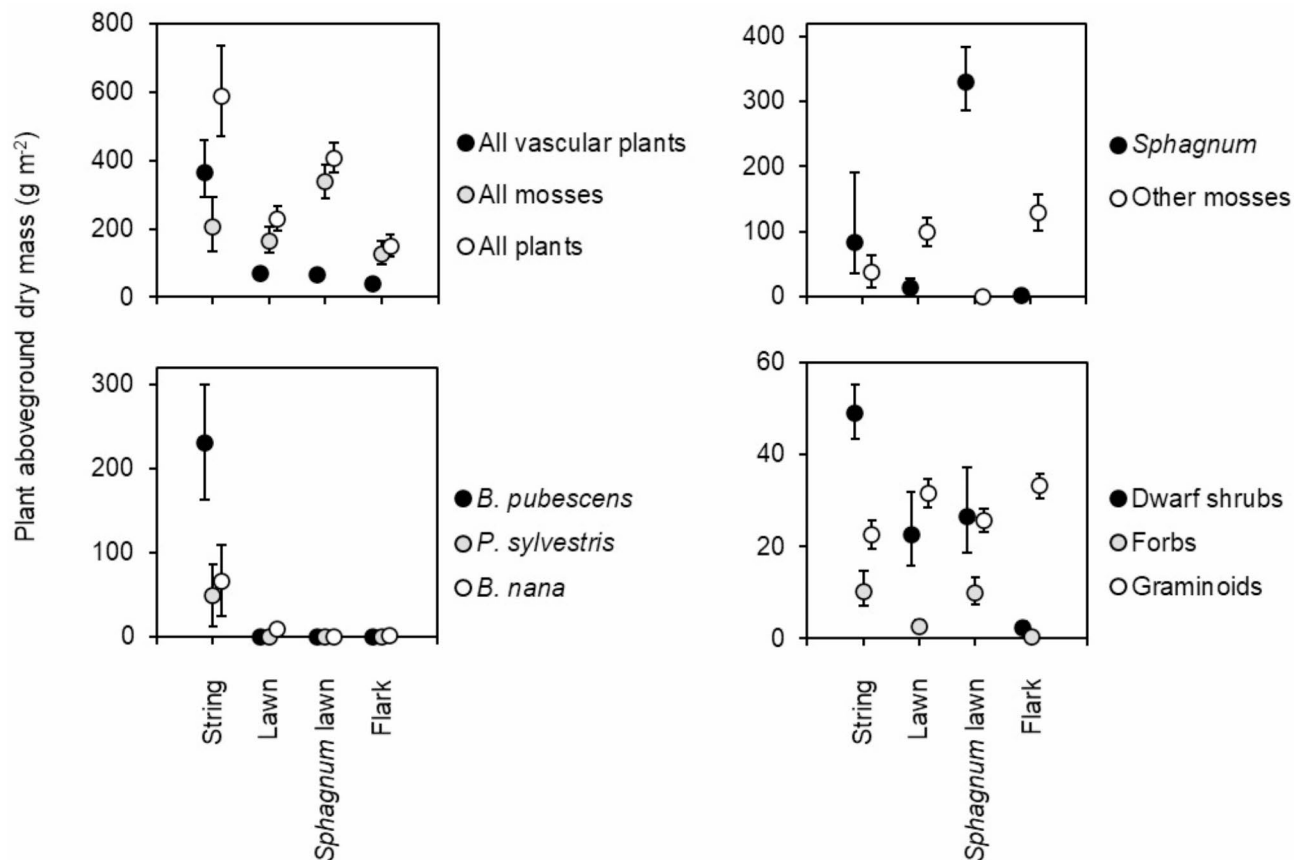


**Fig. 6.** Aboveground biomass (mean  $\pm$  SE) of all vascular plants, all mosses, all plants and the dominant species and functional groups in boreal fen microforms ( $n=7$  for string,  $n=12$  for lawn,  $n=5$  for *Sphagnum* lawn,  $n=24$  for flark; for those variables that were transformed for data analysis, means and standard errors are back-transformed).

than lawn and flark ( $P=0.003$ ), but due to the high moss mass in *Sphagnum* lawn, string and *Sphagnum* lawn did not significantly differ in total plant mass (Fig. 6). The ground layer vascular plant LAI was highest in string ( $0.78 \pm 0.14 \text{ m}^2 \text{ m}^{-2}$ , mean  $\pm$  SE,  $n=7$ ), intermediate in lawn ( $0.51 \pm 0.10 \text{ m}^2 \text{ m}^{-2}$ ,  $n=12$ ) and *Sphagnum* lawn ( $0.49 \pm 0.09 \text{ m}^2 \text{ m}^{-2}$ ,  $n=5$ ), and lowest in flark ( $0.26 \pm 0.03 \text{ m}^2 \text{ m}^{-2}$ ,  $n=24$ ) ( $P<0.001$ ).

No fertility zone effect appeared in the MANOVA multivariate test ( $P=0.232$ ), but the dry mass of mosses ( $P=0.006$  for total moss,  $P=0.010$  for other moss) and all plants ( $P=0.005$ ) varied significantly among the fertility zones in the univariate tests (see complete statistics in Supplementary Table 5). The dry mass of other mosses was higher in the eutrophic zone ( $210 \pm 73 \text{ g m}^{-2}$ ,  $n=5$ ) than in the mesotrophic ( $96 \pm 24 \text{ g m}^{-2}$ ,  $n=25$ ) and oligotrophic ( $61 \pm 14 \text{ g m}^{-2}$ ,  $n=18$ ) zones, and the total dry mass of mosses was higher in the eutrophic ( $320 \pm 82 \text{ g m}^{-2}$ ) and mesotrophic zones ( $269 \pm 41 \text{ g m}^{-2}$ ) than in the oligotrophic zone ( $101 \pm 18 \text{ g m}^{-2}$ ). Total dry mass of all plants followed the same trend, with higher biomass in the eutrophic ( $403 \pm 77 \text{ g m}^{-2}$ ) and mesotrophic zones ( $429 \pm 65 \text{ g m}^{-2}$ ) than in the oligotrophic zone ( $161 \pm 24 \text{ g m}^{-2}$ ). The fertility zone effect on dwarf shrub dry mass was only marginally significant ( $P=0.076$ ), but the trend was the same, i.e. a higher biomass in the eutrophic ( $47 \pm 20 \text{ g m}^{-2}$ ) than oligotrophic zone ( $18 \pm 6 \text{ g m}^{-2}$ ) with an intermediate mass in the mesotrophic zone ( $27 \pm 5 \text{ g m}^{-2}$ ). *Sphagnum*, forb, graminoid and total vascular plant mass and the ground layer vascular plant LAI (Supplementary Fig. 2) did not statistically significantly differ among the fertility zones (Supplementary Table 5). Fertility effects on trees and *B. nana* could not be tested due to a shortage of eutrophic and oligotrophic string plots (Supplementary Table 2).

### Soil properties

MANOVA multivariate test found a highly significant ( $P<0.001$ ) general microform effect on soil properties (Fig. 7) in both soil layers (see complete statistics in Supplementary Table 6). In the upper, 0–5 cm soil layer (which includes plant litter), *Sphagnum* lawn and flark formed the two extremes for all measured variables: while *Sphagnum* lawn had the highest water concentration and lowest bulk density, C and N concentrations and C and N contents, flark had the lowest water concentration and highest bulk density, C and N concentrations and C and N contents (Fig. 7). String and lawn were always between the two extremes and did not differ from each other for any measured variable (Fig. 7). In the deeper, 15–20 cm soil layer, the pattern was different: string had lower water content and higher bulk density, C and N concentrations and C and N contents than flark, lawn and

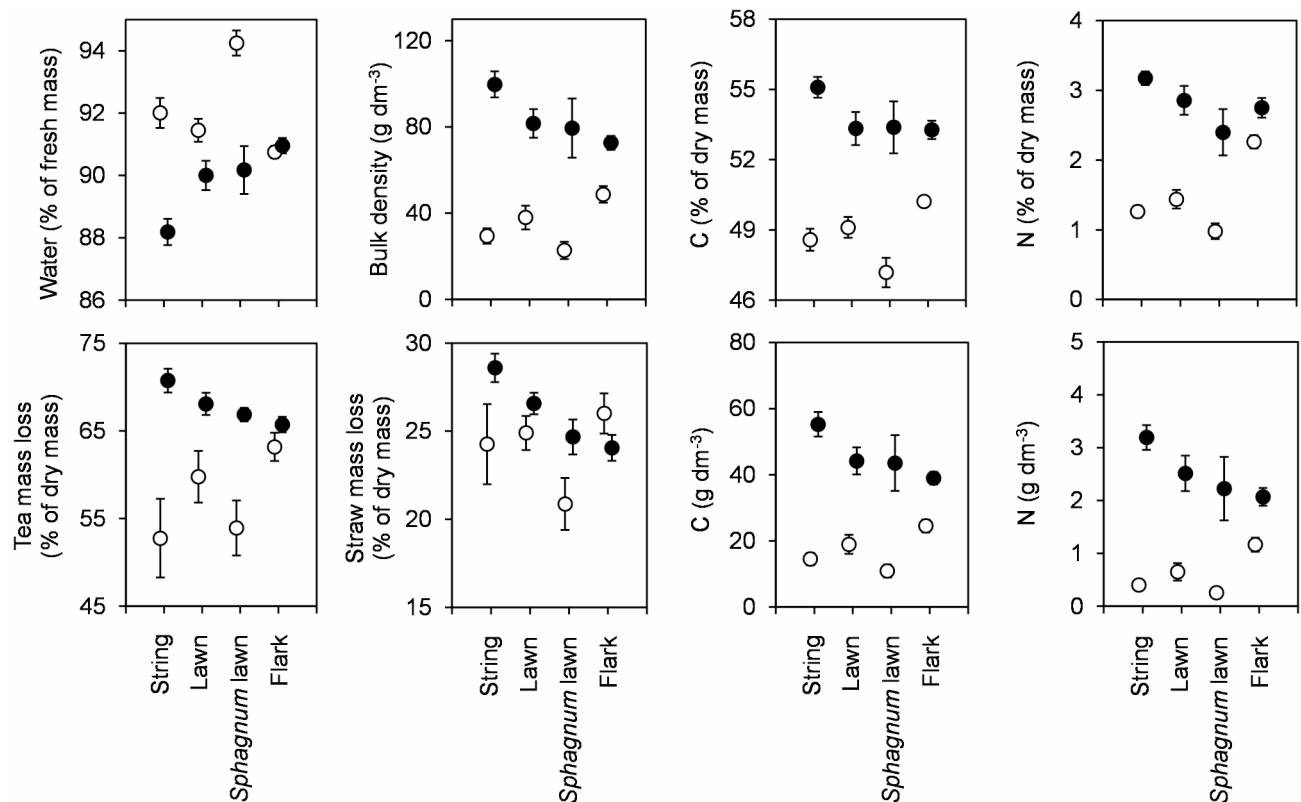


**Fig. 7.** Attributes of soil 0–5 cm layer (open symbols; includes plant litter) and 15–20 cm layer (black symbols) (mean  $\pm$  SE, back-transformed from log-transformed data) and mass loss of tea and straw in bags placed on soil surface (open symbols) and at the depth of 10 cm (black symbols) in boreal fen microforms ( $n = 18$  for string,  $n = 17$  for lawn,  $n = 9$  for *Sphagnum* lawn,  $n = 27$  for flark).

*Sphagnum* lawn, which did not differ from each other for any variable (Fig. 7). Soil pH was on average  $5.0 \pm 0.28$  (mean  $\pm$  SD,  $n = 76$ ) and did not differ among the microforms ( $P = 0.203$ ).

Fertility zone effects on soil properties were rare and the MANOVA multivariate test found a fertility zone effect ( $P = 0.017$ ) in the upper layer only (Supplementary Table 6). In this layer, the eutrophic zone had lower soil N concentration ( $1.43 \pm 0.14\%$  of dry mass, mean  $\pm$  SE,  $n = 19$ ) than the mesotrophic ( $1.84 \pm 0.10\%$ ,  $n = 25$ ) and oligotrophic ( $1.79 \pm 0.16\%$ ,  $n = 23$ ) zones ( $P = 0.017$ ), as well as lower N content ( $0.57 \pm 0.13$  g dm $^{-3}$ ) than the mesotrophic ( $0.88 \pm 0.11$  g dm $^{-3}$ ) and oligotrophic ( $0.83 \pm 0.17$  g dm $^{-3}$ ) zones ( $P = 0.032$ ). Soil C concentration was significantly lower in the eutrophic ( $53.0 \pm 0.5\%$ ) than oligotrophic zone ( $54.9 \pm 0.4\%$ ) in the deeper layer ( $P = 0.019$ ), with the mesotrophic zone having intermediate values ( $53.8 \pm 0.5\%$ ). The pH did not significantly differ among the fertility zones ( $P = 0.073$ ).

Soil properties were strongly correlated within soil layers (Supplementary Table 7a), but weakly or not at all correlated between the layers (Supplementary Table 7b). Upper soil layer C content correlated negatively with total moss mass ( $r = -0.49$ ,  $P < 0.001$ ), whereas the lower layer soil C content correlated positively with total vascular plant mass ( $r = 0.30$ ,  $P < 0.05$ ) and ground layer vascular plant LAI ( $r = 0.41$ ,  $P < 0.01$ ) (see further statistics in Supplementary Table 8).

### Litter decomposition

When placed on the ground, tea had a marginally higher mass loss in flark than string ( $P = 0.057$ ) (Fig. 7) and significantly lower mass loss in the eutrophic ( $55.1 \pm 3.4\%$ ,  $n = 5$ ) and mesotrophic ( $57.3 \pm 2.0\%$ ,  $n = 25$ ) zones than in the oligotrophic zone ( $64.7 \pm 1.9\%$ ,  $n = 18$ ) ( $P = 0.044$ ). At the depth of 10 cm, fertility had no effect on litter mass loss (Supplementary Table 6), but straw had significantly higher mass loss ( $P = 0.011$ ) and tea marginally higher mass loss ( $P = 0.058$ ) in string than flark and *Sphagnum* lawn (Fig. 7).

Tea mass loss and straw mass loss correlated positively ( $r = 0.40$ ,  $P < 0.01$ ) when the bags were buried, but not when the bags were placed on the ground (Supplementary Table 7a). There was neither correlation between the mass loss of litter placed on the ground and the mass loss of litter buried in the soil (Supplementary Table 7b). Tea mass loss was negatively correlated with total moss mass ( $r = -0.29$ ,  $P < 0.05$ ), total vascular plant mass ( $r = -0.40$ ,  $P < 0.01$ ) and ground layer vascular LAI ( $r = -0.34$ ,  $P < 0.05$ ) when the bags were placed on the ground, whereas straw mass loss was positively correlated with total vascular plant mass ( $r = 0.46$ ,  $P < 0.01$ ) and ground layer vascular LAI ( $r = 0.38$ ,  $P < 0.01$ ) when the bags were buried in the soil (see further statistics in Supplementary Table 8).



## Discussion

Our main objective was to examine the relative role of fertility and microtopography as CO<sub>2</sub> and CH<sub>4</sub> exchange drivers in a fen ecosystem. Our chamber measurements show that higher fertility led to greater fluxes in both gases: the eutrophic zone had around double daytime NEE<sub>1200</sub>, GPP<sub>1200</sub>, R<sub>e</sub> and CH<sub>4</sub> emissions in comparison to the oligotrophic zone. In contrast, the microform effect differed between the gases: string had higher NEE<sub>1200</sub>, GPP<sub>1200</sub> and R<sub>e</sub>, respectively, than *Sphagnum* lawn and flark, whereas *Sphagnum* lawn had higher CH<sub>4</sub> emissions than string and flark. These results show that while CO<sub>2</sub> and CH<sub>4</sub> exchange are closely coupled across the fertility gradient, the coupling is broken by microtopography. Overall, it appears that the relative importance of microtopography and fertility differ between the two gases: while microform explained 31–39% and fertility 10–15% of total variation in CO<sub>2</sub> exchange, microform explained 14% and fertility 36% of variation in CH<sub>4</sub> exchange.

### Fertility and CO<sub>2</sub> and CH<sub>4</sub> exchange

The increasing CO<sub>2</sub> and CH<sub>4</sub> exchange that we found with increasing fertility is an indication of higher fertility sustaining higher plant production and biomass. In line with this assumption, we found that the dry masses of other mosses, all mosses, dwarf shrubs and all plants were significantly higher in the eutrophic than in the oligotrophic zone. Although many vegetation variables, including vascular plant LAI and *Sphagnum* biomass, did not significantly differ among the fertility zones, the results for all mosses and all plants show that higher fertility was in general associated with greater primary production. Considering that leaf area governs the magnitude of plant CO<sub>2</sub> exchange and GPP and should readily respond to soil fertility, it was unexpected that vascular plant LAI was one of the variables that were not statistically significantly associated with soil fertility. This finding is, however, likely a result of insufficient sample size and statistical power rather than a true pattern in the fen as the mean of LAI in the eutrophic and mesotrophic zones was, after all, higher than the mean of LAI in the oligotrophic zone (Supplementary Fig. 2).

The variation of soil variables along the fertility gradient further supports the idea that vegetation structure was affected by fertility. Plant species adapted to poor soils typically produce recalcitrant litter that is hard to decompose<sup>44,45</sup>. In less fertile soils, therefore, litter decomposition is slow, which leads to accumulation of organic C and N in the soil<sup>46</sup>. In our study site, the soil in the eutrophic zone had lower N concentration than the soil in the oligotrophic zone. This is an indication of faster litter decomposition, faster N cycling and a bigger proportion of total N being taken-up into plant biomass in the eutrophic zone. The mass loss of standard litter materials, tea leaves and straw, was not affected by the fertility zone when the litter bags were placed in the peat, showing that microbes were equally efficient in litter decomposition across the fertility gradient. This suggests that the observed differences in peat N concentration among the fertility zones were not due to differences in the efficiency of the decomposers but rather, due to differences in the decomposability of the litter produced in different zones. In line with this reasoning, Myers et al.<sup>47</sup> found that microbial basal respiration and substrate induced respiration (SIR), the proxies of microbial activity and biomass, did not differ between poor and rich fens. Also, in a mesocosm study, peat N availability did not affect tea decomposition and only slightly affected the decomposition rate of *Carex* shoot and root material<sup>26</sup>.

Primary production is known to be closely associated with CH<sub>4</sub> emissions in various spatial scales ranging from single peatlands<sup>7</sup> and Arctic tundra and wetland sites<sup>48</sup> to global scale<sup>49</sup>. The positive association of GPP with CH<sub>4</sub> release is typically governed by both greater labile C source for methanogens and by transport of CH<sub>4</sub> through plant tissues<sup>48,50</sup>. The contribution of peat C to CH<sub>4</sub> emissions is small<sup>51</sup>. Supporting this common insight, fertility had a clear positive effect on both GPP<sub>1200</sub> and daytime CH<sub>4</sub> efflux in our study and explained as much as 36% of total variation in CH<sub>4</sub> exchange. That microtopography only explained 14% of the variation further supports the view that CH<sub>4</sub> production rather than CH<sub>4</sub> oxidation in upper soil layers controlled the CH<sub>4</sub> exchange.

### Microtopography and CO<sub>2</sub> and CH<sub>4</sub> exchange

Consistent with our finding that microform explained 31–39% of total variation in CO<sub>2</sub> exchange, the differences in CO<sub>2</sub> fluxes between the microforms were associated with microform differences in vegetation and soil attributes. NEE<sub>1200</sub>, GPP<sub>1200</sub> and R<sub>e</sub> were higher in string than flark and *Sphagnum* lawn, which apparently is a consequence of vascular plant LAI and the biomass of plant functional groups, except for mosses and graminoids, having higher values in string. This finding contributes to the common understanding that strings have higher vascular plant LAI, GPP and R<sub>e</sub> than flarks<sup>7,8,12,13,15</sup>. The CO<sub>2</sub> exchange of lawns instead seems to depend on the plant species composition in the lawn: for instance, Riutta et al.<sup>13</sup> found that *Carex lasiocarpa* (Ehrh.) lawns had higher GPP and *Carex rostrata* (Stokes) and *Eriophorum vaginatum* (L.) lawns lower GPP than the strings, while all lawns had higher GPP than the flarks. In our study, *Sphagnum* lawn had higher vascular plant LAI, higher biomass of dwarf shrubs, forbs, and *Sphagnum* mosses than flark, but the values of NEE<sub>1200</sub>, GPP<sub>1200</sub> and R<sub>e</sub> remained close to those measured in flark.

In addition to the higher plant biomass and LAI, which govern the higher GPP and partially also R<sub>e</sub>, our data reveal soil attributes that likely contributed to higher R<sub>e</sub> in string. When buried in the peat, both straw and tea had statistically significantly higher mass loss in string than in flark and *Sphagnum* lawn, showing that decomposition of plant litter, whether easily degradable (tea) or more recalcitrant (straw), is fastest in string soil. This finding differs from earlier results in a nutrient-poor fen, where the decomposition rate of plant litter did not differ between strings and flarks<sup>52</sup>. We also found that straw mass loss, when buried in the peat, was positively correlated with aboveground vascular plant dry mass. This finding is probably because vascular plant roots can accelerate organic matter decomposition in peat through releasing oxygen, which enhances aerobic decomposition<sup>53</sup>, and through releasing labile C compounds, which induce microbial priming of N from plant litter<sup>54–56</sup>. Finally, the lower layer soil C content correlated positively with total vascular plant mass and ground

layer vascular LAI, which is an indication that vascular plant roots bring and store C in deeper layers of soil. As total vascular plant aboveground biomass was remarkably higher in string than other microforms, these effects and processes were apparently strongest in string.

In fens,  $\text{CH}_4$  flux is often positively correlated with the abundance of graminoids as these plants can bypass  $\text{CH}_4$  through the oxic upper layers of peatlands<sup>20</sup>. Our results do not obey this generalization since *Sphagnum* lawn had on average 35% higher daytime  $\text{CH}_4$  emissions than both flark and string although graminoid biomass was not higher in *Sphagnum* lawn than in other microforms. The explanation may be that *Menyanthes trifoliata* (L.), which also has a high  $\text{CH}_4$  transport rate<sup>57</sup>, was common on lawns in our study site, covering up to 20%. Consistent with our results, Dinsmore et al.<sup>58</sup> found in the same fen that  $\text{CH}_4$  emissions and *Sphagnum* cover were positively associated. Some earlier studies have in turn found equal  $\text{CH}_4$  emissions in lawns and flarks<sup>13,59</sup>. Overall, the microform was not very important in governing the  $\text{CH}_4$  exchange in our fen as it only explained 14% of the total variation.

What is notable in our soil data is that the characteristics of the upper (0–5 cm) and lower (15–20 cm) layers of soil, as well as the decomposition of litter on the ground and in the soil, correlated weakly at best. When excluding *Sphagnum* lawn from the comparison, the string-lawn-flark continuum reversed for all soil variables between the upper and lower soil layers. This means that while the microforms have characteristic soils in both upper and lower layers, differences among microforms are not predictable from one layer to another. Within soil layers, however, all peat attributes correlated strongly with each other, suggesting that easily achievable variables like bulk density are sufficient for predicting the variation of, for instance, soil C concentration and C content across the fen landscape. As an exception though, decomposer activity and litter mass loss seem to follow vegetation structure rather than peat characteristics.

### Temperature, water table level and $\text{CO}_2$ and $\text{CH}_4$ exchange

It is well established that peatland  $\text{CO}_2$  and  $\text{CH}_4$  exchange are sensitive to changes in temperature and WTL. For instance, annual NEE and annual mean temperature are positively correlated across northern hemisphere peatlands<sup>60</sup> and lowering WTL leads to a decline in  $\text{CH}_4$  emissions<sup>50</sup>. In our study, the three growing seasons differed in air temperature and precipitation, which caused differences in growing season temperature sum, soil temperature and WTL across the years. The temperature sum was ca. 200 DD lower, the June–August air temperature 2 °C lower and the soil temperature (at 10 cm depth) 4 °C lower in 2015 than in 2014 and 2016. Precipitation was in turn lowest in 2014 and highest in 2016, leading to gradually increasing WTL across the 2014–2016 sequence from on average 7.5 cm below surface in summer 2014 to on average 0.4 cm above surface in summer 2016. Since temperature and precipitation did not correlate across the years, their effects on  $\text{CO}_2$  and  $\text{CH}_4$  exchange could be disentangled.

Comparing the EC estimates of gas fluxes with summer weather across the three study years suggests that  $\text{GPP}_{1200}$  was strongly controlled by temperature:  $\text{GPP}_{1200}$  was lower (i.e. plant production was higher) in warmer summers 2014 and 2016 than in the cooler summer 2015, and despite the contrasting WTL in 2014 and 2016, mean  $\text{GPP}_{1200}$  did not differ between 2014 and 2016. All other fluxes seemed to be affected by both temperature and WTL.  $R_e$  was higher in warmer summers 2014 and 2016 than in the cooler summer 2015, but also higher in 2014 than in 2016, suggesting that lower WTL and deeper oxic layer were associated with higher  $R_e$ .  $\text{NEE}_{1200}$  was stronger in warmer summers 2014 and 2016 than in 2015, which shows that higher temperatures increased  $\text{GPP}_{1200}$  relatively more than  $R_e$ . Similarly, Lindroth et al.<sup>60</sup> reported that  $\text{GPP}$  was more sensitive to temperature than  $R_e$  in four bogs and fens along a 56°N–69°N latitude gradient in northern Europe, thus suggesting higher  $\text{CO}_2$  capture in peatlands under increasing temperatures.  $\text{NEE}_{1200}$  was also stronger in 2016 than in 2014, suggesting that higher WTL in 2016 produced higher  $\text{NEE}_{1200}$ , apparently due to lower  $R_e$ . Similarly, in a nine-year data of a northern fen, wet years had higher NEE than dry years<sup>61</sup>.

Our EC data show that, following the pattern in  $\text{GPP}_{1200}$ ,  $\text{CH}_4$  emissions were higher in the warmer summers 2014 and 2016 than in 2015. This is in line with the understanding that  $\text{CH}_4$  production in peat is controlled by temperature and plant photosynthate availability<sup>50,62</sup>.  $\text{CH}_4$  emissions were also clearly higher in 2016 with high WTL than in 2014 with low WTL, which contributes to the common view that the net  $\text{CH}_4$  flux is limited by methanotroph oxidation in the oxic peat and moss layers<sup>20,50,61</sup>.

Earlier research suggests that gas flux responses to changes in temperature and WTL may also differ between microforms. For instance, Alm et al.<sup>7</sup> concluded that string C exchange was most sensitive to weather variation. Our measurements provide evidence that temperature and precipitation can modify both microform and fertility effects. First, chamber daytime  $\text{CH}_4$  emissions from *Sphagnum* lawn were 34%, 22% and 45% higher than emissions from flark and string in 2014, 2015 and 2016, respectively, suggesting that differences between microforms in  $\text{CH}_4$  emissions increased with increasing temperature (2014 and 2016 were warmer than 2015) and increasing WTL (2016 had higher WTL than 2014). Second,  $\text{CH}_4$  emissions from the eutrophic zone were 145%, 55% and 84% higher than emissions from mesotrophic and oligotrophic zones in 2014, 2015 and 2016, respectively, thus suggesting that differences between fertility zones increased with increasing temperature and decreasing WTL. Responses of abiotic variables also varied as differences in soil temperature between microforms increased with increasing air temperature. Lastly, it is noteworthy that differences in mean daytime soil temperatures between the years were double to differences in mean air temperatures, suggesting that daytime soil processes are subjected to much larger amplitude of temperature variation than the air temperature variation.

### *Sphagnum* effect on lawn attributes

*Sphagnum* expansion is supposed to slow down decomposition and enhance C accumulation in northern fens, eventually transforming fens into bogs<sup>22,28</sup>. We investigated the effects of *Sphagnum* abundance by comparing the attributes of lawn and *Sphagnum* lawn. Differences between these two lawns could be traced to differences

in their moss composition and biomass as *Sphagnum* lawn had no other mosses and double moss biomass in comparison to lawn. Vascular plant LAI and total vascular plant biomass were similar in both lawns, and of the vascular plants, only forbs differed in biomass between the two lawns. The effect of *Sphagnum* dominance on soil attributes was visible in the upper soil layer (0–5 cm), where *Sphagnum* lawn had higher water concentration and lower bulk density and C and N content than lawn. *Sphagnum* mosses can increase peatland N accumulation through sustaining atmospheric N<sub>2</sub> fixation by methanotrophic and other bacteria<sup>63,64</sup>. We did not find evidence that this process would increase peat N concentration or N content, however, as these attributes were lower under *Sphagnum* lawn than lawn. At the depth of 10 cm, the mass loss of both tea and straw was lower under *Sphagnum* lawn than string but did not differ between lawn and string. This pattern is likely a consequence of *Sphagnum* litter being a hostile environment for decomposers. *Sphagnum* mosses can produce organic compounds that acidify the soil environment and have negative influence on soil microbes<sup>50</sup>. Deeper in the soil (15–20 cm), soil attributes did not differ between the two lawns, which suggests that the influence of intensive *Sphagnum* coverage on peat attributes is limited to the upper soil layers.

## Conclusions

Our results suggest that besides being affected by variation in temperature, microtopography and hydrology, growing season GHG fluxes in fens are also significantly affected by variation in fertility. Within our northern boreal fen, primary production and CO<sub>2</sub> exchange increase with increasing fertility, and daytime CH<sub>4</sub> emissions are more closely associated with fertility than microtopography. It further appears that the difference between oligotrophic and eutrophic fen sites in growing season daytime CH<sub>4</sub> emissions increases with increasing growing season temperature. This indicates that the relative role of fertile fen sites in peatland CH<sub>4</sub> emissions will increase in future higher temperatures.

## Data availability

The datasets generated during and/or analyzed during the current study are available from the corresponding author on reasonable request.

Received: 25 September 2024; Accepted: 17 February 2025

Published online: 12 March 2025

## References

1. Yu, Z., Loisel, J., Brosseau, D. P., Beilman, D. W. & Hunt, S. J. Global peatland dynamics since the last glacial Maximum. *Geophys. Res. Lett.* **37**, L13402. <https://doi.org/10.1029/2010GL043584> (2010).
2. Harden, J. W., Mark, R. K., Sundquist, E. T. & Stallard, R. F. Dynamics of soil carbon during deglaciation of the Laurentide ice sheet. *Science* **258**, 1921–1924 (1992). <https://www.jstor.org/stable/2880469>
3. Treat, C. C. et al. Widespread global peatland establishment and persistence over the last 130,000 y. *PNAS* **116**, 4822–4827. <https://doi.org/10.1073/pnas.1813305116> (2019).
4. Belyea, L. R. & Clymo, R. S. Feedback control of the rate of peat formation. *Proc. R. Soc. Lond. B.* **268**, 1315–1321 (2001).
5. Harris, L. I., Roulet, N. T. & Moore, T. R. Mechanisms for the development of microform patterns in peatlands of the Hudson Bay Lowland. *Ecosystems* **23**, 741–767. <https://doi.org/10.1007/s10021-019-00436-z> (2020).
6. Turunen, J., Tomppo, E., Tolonen, K. & Reinikainen, A. Estimating carbon accumulation rates of undrained mires in Finland - application to boreal and subarctic regions. *Holocene* **12**, 69–80. <https://doi.org/10.1191/0959683602hl522rp> (2002).
7. Alm, J. et al. Reconstruction of the carbon balance for microsites in a boreal oligotrophic pine fen, Finland. *Oecologia* **110**, 423–431. <https://doi.org/10.1007/s004420050177> (1997).
8. Heiskanen, L. et al. Carbon dioxide and methane exchange of a patterned subarctic fen during two contrasting growing seasons. *Biogeosciences* **18**, 873–896. <https://doi.org/10.5194/bg-18-873-2021> (2021).
9. Griffiths, T. J., Rouse, W. R. & Waddington, J. M. Interannual variability of net ecosystem CO<sub>2</sub> exchange at a subarctic fen. *Global Biogeochem. Cy.* **14**, 1109–1121. <https://doi.org/10.1029/1999GB001243> (2000).
10. Shurpali, N. J., Verma, S. B., Kim, J. & Arkebauer, T. J. Carbon dioxide exchange in a peatland ecosystem. *J. Geophys. Res.-Atmos.* **100**, 14319–14326. <https://doi.org/10.1029/95JD01227> (1995).
11. Andrus, R. E., Wagner, D. J. & Titus, J. E. Vertical zonation of *Sphagnum* mosses along hummock-hollow gradients. *Can. J. Bot.* **61**, 3128–3139. <https://doi.org/10.1139/b83-352> (1983).
12. Purre, A.-H. et al. Carbon dioxide fluxes and vegetation structure in rewetted and pristine peatlands in Finland and Estonia. *Boreal Environ. Res.* **24**, 243–261 (2019).
13. Riutta, T. et al. Spatial variation in plant community functions regulates carbon gas dynamics in a boreal fen ecosystem. *Tellus B.* **59**, 838–852. <https://doi.org/10.1111/j.1600-0889.2007.00302.x> (2007).
14. Heikkinen, J. E. P., Maljanen, M., Aurela, M., Hargreaves, K. J. & Martikainen, P. J. Carbon dioxide and methane dynamics in a sub-arctic peatland in northern Finland. *Polar Res.* **21**, 49–62. <https://doi.org/10.3402/polar.v21i1.6473> (2002).
15. Bubier, J. L., Crill, P. M., Moore, T. R., Savage, K. & Varner, R. K. Seasonal patterns and controls on net ecosystem CO<sub>2</sub> exchange in a boreal peatland complex. *Global Biogeochem. Cy.* **12**, 703–714. <https://doi.org/10.1029/98GB02426> (1998).
16. Moore, T. R., Bubier, J. L. & Bledzki, L. Litter decomposition in temperate peatland ecosystems: the effect of substrate and site. *Ecosystems* **10**, 949–963. <https://doi.org/10.1007/s10021-007-9064-5> (2007).
17. Wheeler, B. D. & Proctor, M. C. F. Ecological gradients, subdivisions and terminology of north-west European mires. *J. Ecol.* **88**, 187–203. <https://doi.org/10.1046/j.1365-2745.2000.00455.x> (2000).
18. Chapin, C. T., Bridgman, S. D. & Pastor, J. pH and nutrient effects on above-ground net primary production in a Minnesota, USA bog and fen. *Wetlands* **24**, 186–201. [https://doi.org/10.1672/0277-5212\(2004\)024\[0186:PANEOA\]2.0.CO;2](https://doi.org/10.1672/0277-5212(2004)024[0186:PANEOA]2.0.CO;2) (2004).
19. Gerdol, R., Siffi, C. & Bombonato, L. Aboveground production and nutrient status of the vegetation of different mire types in the South-eastern Alps (Italy). *Bot. Helv.* **120**, 85–93. <https://doi.org/10.1007/s00035-010-0077-x> (2010).
20. Turetsky, M. R. et al. A synthesis of methane emissions from 71 northern, temperate, and subtropical wetlands. *Glob Change Biol.* **20**, 2183–2197. <https://doi.org/10.1111/gcb.12580> (2014).
21. Loisel, J. & Bunsen, M. Abrupt fen-bog transition across southern Patagonia: timing, causes, and impacts on carbon sequestration. *Front. Ecol. Evol.* **8**, 273. <https://doi.org/10.3389/fevo.2020.00273> (2020).
22. Magnan, G. et al. Widespread recent ecosystem state shifts in high-latitude peatlands of northeastern Canada and implications for carbon sequestration. *Glob Change Biol.* **28**, 1919–1934. <https://doi.org/10.1111/gcb.16032> (2022).



23. Wassen, M. J., Barendregt, A., Palczynski, A., de Smidt, J. T. & de Mars, H. The relationship between fen vegetation gradients, groundwater flow and flooding in an undrained valley mire at Biebrza, Poland. *J. Ecol.* **78**, 1106–1122. <https://doi.org/10.2307/2260955> (1990).
24. Wheeler, B. D., Shaw, S. C. & Cook, R. E. D. Phytometric assessment of the fertility of undrained rich-fen soils. *J. Appl. Ecol.* **29**, 466–475. <https://doi.org/10.2307/2404514> (1992).
25. Aerts, R., de Caluwe, H. & Konings, H. Seasonal allocation of biomass and nitrogen in four *Carex* species from mesotrophic and eutrophic fens as affected by nitrogen supply. *J. Ecol.* **80**, 653–664. <https://doi.org/10.2307/2260857> (1992).
26. Hinzke, T. et al. Potentially peat-forming biomass of fen sedges increases with increasing nutrient levels. *Funct. Ecol.* **35**, 1579–1595. <https://doi.org/10.1111/1365-2435.13803> (2021).
27. Godin, A., McLaughlin, J. W., Webster, K. L., Packalen, M. & Basiliko, N. Methane and methanogen community dynamics across a boreal peatland nutrient gradient. *Soil. Biol. Biochem.* **48**, 96–105. <https://doi.org/10.1016/j.soilbio.2012.01.018> (2012).
28. Granlund, L. et al. Recent lateral expansion of *Sphagnum* bogs over central fen areas of boreal aapa mire complexes. *Ecosystems* **25**, 1455–1475. <https://doi.org/10.1007/s10021-021-00726-5> (2022).
29. Euroala, S., Bendiksen, K. & Rönkä, A. Suokasviopas, 2nd ed. (Guide to mire plants, in Finnish). *Oulanka Rep.* **9**, 205–pp (1992).
30. Laine, J. et al. The intricate beauty of *Sphagnum* mosses - a Finnish guide to identification. University of Helsinki, Department of Forest Ecology Publications 39:1–190. (2009).
31. Laitinen, J. et al. Mire systems in Finland – special view to aapa mires and their water-flow pattern. *Suo* **58**, 1–26 (2007).
32. Jokinen, P. et al. Tilastoja Suomen ilmastosta ja merestä 1991–2020 (Climatological and oceanographic statistics of Finland 1991–2020, in Finnish with an abstract in English). Finnish Meteorological Institute Reports 2021:8. (2021).
33. Räsänen, A. et al. Detecting northern peatland vegetation patterns at ultra-high spatial resolution. *Remote Sens. Ecol. Conserv.* **6**, 457–471. <https://doi.org/10.1002/rse2.140> (2020).
34. Chapin, III F. S., Bret-Harte, M. S., Hobbie, S. E. & Zhong, H. Plant functional types as predictors of transient responses of arctic vegetation to global change. *J. Veg. Sci.* **7**, 347–358. <https://doi.org/10.2307/3236278> (1996).
35. Starr, M., Hartman, M. & Kinnunen, T. Biomass functions for mountain birch in the Vuoskojärvi integrated monitoring area. *Boreal Environ. Res.* **3**, 297–303 (1998).
36. Varmola, M. & Vuokila, E. Pienten mäntyjen tilavuusyhtälöt ja -taulukot. Summary: tree volume functions and tables for small-sized pines. *Folia for.* **652**, 1–24. <http://urn.fi/URN:ISBN:951-40-0735-2>. (1986).
37. Kauppi, P., Tomppo, E. & Ferm, A. C and N storage in living trees within Finland since 1950s. *Plant Soil.* **168–169**, 633–638. <https://doi.org/10.1007/BF00029377> (1995).
38. Keuskamp, J. A., Dingemans, B. J. J., Lehtinen, T., Sarneel, J. M. & Hefting, M. H. Tea bag index: a novel approach to collect uniform decomposition data across ecosystems. *Methods Ecol. Evol.* **4**, 1070–1075. <https://doi.org/10.1111/2041-210X.12097> (2013).
39. Silfver, T. et al. Insect herbivory dampens subarctic birch forest C sink response to warming. *Nat. Commun.* **11**, 2529. <https://doi.org/10.1038/s41467-020-16404-4> (2020).
40. Laurila, T. et al. Seasonal variations of net CO<sub>2</sub> exchange in European Arctic ecosystems. *Theor. Appl. Climatol.* **70**, 183–201. <https://doi.org/10.1007/s007040170014> (2001).
41. Whiting, G. J. CO<sub>2</sub> exchange in the Hudson Bay lowlands: community characteristics and multispectral reflectance properties. *J. Geophys. Res.* **99**, 1519–1528. <https://doi.org/10.1029/93JD01833> (1994).
42. Aubinet, M., Vesala, T. & Papale, D. *Eddy Covariance: A Practical Guide to Measurement and Data Analysis* (Springer Netherlands, 2012).
43. Aurela, M. et al. Carbon dioxide exchange on a northern boreal fen. *Boreal Environ. Res.* **14**, 699–710 (2009).
44. Hobbie, S. E. Effects of plant species on nutrient cycling. *Trends Ecol. Evol.* **7**, 336–339. [https://doi.org/10.1016/0169-5347\(92\)90126-V](https://doi.org/10.1016/0169-5347(92)90126-V) (1992).
45. Hobbie, S. E. Plant species effects on nutrient cycling: revisiting litter feedbacks. *Trends Ecol. Evol.* **30**, 357–363. <https://doi.org/10.1016/j.tree.2015.03.015> (2015).
46. Wardle, D. A., Zackrisson, O., Hörnberg, G. & Gallet, C. The influence of island area on ecosystem properties. *Science* **277**, 1296–1299. <https://doi.org/10.1126/science.277.5330.1296> (1997).
47. Myers, B., Webster, K. L., McLaughlin, J. W. & Basiliko, N. Microbial activity across a boreal peatland nutrient gradient: the role of fungi and bacteria. *Wetlands Ecol. Manage.* **20**, 77–88. <https://doi.org/10.1007/s11273-011-9242-2> (2012).
48. McEwing, K. R., Fisher, J. P. & Zona, D. Environmental and vegetation controls on the spatial variability of CH<sub>4</sub> emission from wet-sedge and tussock tundra ecosystems in the Arctic. *Plant. Soil.* **388**, 37–52. <https://doi.org/10.1007/s11104-014-2377-1> (2015).
49. Whiting, G. J. & Chanton, J. P. Primary production control of methane emission from wetlands. *Nature* **364**, 794–795. <https://doi.org/10.1038/364794a0> (1993).
50. Bridgman, S. D., Cadillo-Quiroz, H., Keller, J. K. & Zhuang, Q. Methane emissions from wetlands: biogeochemical, microbial, and modeling perspectives from local to global scales. *Glob Change Biol.* **19**, 1325–1346. <https://doi.org/10.1111/gcb.12131> (2013).
51. Kuder, T. & Krüge, M. A. Carbon dynamics in peat bogs: insights from substrate macromolecular chemistry. *Global Biogeochem. Cy.* **15**, 721–727. <https://doi.org/10.1029/2000GB001293> (2001).
52. Barreto, C. & Lindo, Z. Drivers of decomposition and the detrital invertebrate community differ across a hummock-hollow microtopology in Boreal peatlands. *Écoscience* **25**, 39–48. <https://doi.org/10.1080/11956860.2017.1412282> (2018).
53. Marschner, P. Processes in submerged soils – linking redox potential, soil organic matter turnover and plants to nutrient cycling. *Plant Soil.* **464**, 1–12. <https://doi.org/10.1007/s11104-021-05040-6> (2021).
54. Craine, J., Morrow, C. & Fierer, N. Microbial nitrogen limitation increases decomposition. *Ecology* **88**, 2105–2113. <https://doi.org/10.1890/06-1847.1> (2007).
55. Kuzyakov, Y., Friedel, J. K. & Stahr, K. Review of mechanisms and quantification of priming effects. *Soil. Biol. Biochem.* **32**, 1485–1498. [https://doi.org/10.1016/S0038-0717\(00\)00084-5](https://doi.org/10.1016/S0038-0717(00)00084-5) (2000).
56. Moorhead, D. L. & Sinsabaugh, R. L. A theoretical model of litter decay and microbial interaction. *Ecol. Monogr.* **76**, 151–174. [https://doi.org/10.1890/0012-9615\(2006\)076\[0151:ATMOLD\]2.0.CO;2](https://doi.org/10.1890/0012-9615(2006)076[0151:ATMOLD]2.0.CO;2) (2006).
57. Ge, M. et al. Plant phenology and species-specific traits control plant CH<sub>4</sub> emissions in a northern boreal Fen. *New. Phytol.* **238**, 1019–1032. <https://doi.org/10.1111/nph.18798> (2023).
58. Dinsmore, K. J. et al. Growing season CH<sub>4</sub> and N<sub>2</sub>O fluxes from a subarctic landscape in northern Finland; from chamber to landscape scale. *Biogeosciences* **14**, 799–815. <https://doi.org/10.5194/bg-14-799-2017> (2017).
59. Heikkinen, J. E. P., Elsakov, V. & Martikainen, P. J. Carbon dioxide and methane dynamics and annual carbon balance in tundra wetland in NE Europe, Russia. *Global Biogeochem. Cy.* **16**, 1115. <https://doi.org/10.1029/2002GB001930> (2002).
60. Lindroth, A. et al. Environmental controls on the CO<sub>2</sub> exchange in north European mires. *Tellus* **59B**, 812–825. <https://doi.org/10.1111/j.1600-0889.2007.00310.x> (2007).
61. Olefeldt, D. et al. A decade of boreal rich fen greenhouse gas fluxes in response to natural and experimental water table variability. *Glob Change Biol.* **23**, 2428–2440. <https://doi.org/10.1111/gcb.13612> (2017).
62. Kettunen, A. Connecting methane fluxes to vegetation cover and water table fluctuations at microsite level: a modeling study. *Global Biogeochem. CY.* **17**, 1051. <https://doi.org/10.1029/2002GB001958> (2003).
63. Larmola, T. et al. Methanotrophy induces nitrogen fixation during peatland development. *PNAS* **111**, 734–739. <https://doi.org/10.1073/pnas.1314284111> (2014).
64. Stuart, J. E. M. et al. Host identity as a driver of moss-associated N<sub>2</sub> fixation rates in Alaska. *Ecosystems* **24**, 530–547. <https://doi.org/10.1007/s10021-020-00534-3> (2021).

## Acknowledgements

We thank Maria Laine and Tiina Heikkinen for assisting with field work and Santeri Savolainen for analyzing soil C and N concentrations. This work was supported by the Academy of Finland (CAPTURE project, grant number 296423).

## Author contributions

The study was conceptualized and designed by T.P., M.A., T.V. and J.M. Data collection and analysis were performed by all authors. The manuscript was composed by J.M. with all authors providing material, review and comments. All authors read and approved the manuscript.

## Declarations

## Competing interests

The authors declare no competing interests.

## Additional information

**Supplementary Information** The online version contains supplementary material available at <https://doi.org/10.1038/s41598-025-90845-z>.

**Correspondence** and requests for materials should be addressed to J.M.

**Reprints and permissions information** is available at [www.nature.com/reprints](http://www.nature.com/reprints).

**Publisher's note** Springer Nature remains neutral with regard to jurisdictional claims in published maps and institutional affiliations.

**Open Access** This article is licensed under a Creative Commons Attribution-NonCommercial-NoDerivatives 4.0 International License, which permits any non-commercial use, sharing, distribution and reproduction in any medium or format, as long as you give appropriate credit to the original author(s) and the source, provide a link to the Creative Commons licence, and indicate if you modified the licensed material. You do not have permission under this licence to share adapted material derived from this article or parts of it. The images or other third party material in this article are included in the article's Creative Commons licence, unless indicated otherwise in a credit line to the material. If material is not included in the article's Creative Commons licence and your intended use is not permitted by statutory regulation or exceeds the permitted use, you will need to obtain permission directly from the copyright holder. To view a copy of this licence, visit <http://creativecommons.org/licenses/by-nc-nd/4.0/>.

© The Author(s) 2025